Organic Electronics 13 (2012) 1245–1249

Contents lists available at SciVerse ScienceDirect

Organic Electronics

journal homepage: www.elsevier.com/locate/orgel

Improved power efficiency in deep blue phosphorescent organic light-emitting diodes using an acridine core based hole transport material

Mounggon Kim, Jun Yeob Lee *

Department of Polymer Science and Engineering, Dankook University, Jukjeon-dong, Suji-gu, Yongin-si, Gyeonggi-do 448-701, Republic of Korea

ARTICLE INFO

Article history:
Received 2 February 2012
Received in revised form 19 March 2012
Accepted 24 March 2012
Available online 17 April 2012

Keywords:
Acridine core
Hole transport material
High efficiency
High triplet energy

ABSTRACT

A high triplet energy hole transport material with an acridine core was synthesized as the hole transport material for deep blue phosphorescent organic light emitting diodes. The acridine core based hole transport material showed a high triplet energy of 2.89 eV for efficient triplet exciton blocking and highest occupied molecular orbital of 5.96 eV for efficient hole injection in deep blue phosphorescent organic light-emitting diodes. The acridine core based hole transport material showed low driving voltage than common high triplet energy hole transport material and power efficiency of deep blue phosphorescent organic light-emitting diodes was improved by more than 50%.

© 2012 Elsevier B.V. All rights reserved.

1. Introduction

The device performances of deep blue phosphorescent organic light-emitting diodes (PHOLEDs) depends on charge transport materials and emitting materials. Although the emitting materials mostly determine light emitting performances of PHOLEDs, the charge transport materials are also critical to the device performances of PHOLEDs.

Hole transport materials (HTMs) in PHOLEDs are required to possess high triplet energy for triplet exciton blocking, highest occupied molecular orbital (HOMO) level for hole injection and lowest unoccupied molecular orbital (LUMO) level for electron blocking. In particular, the triplet energy of HTM should be higher than that of phosphorescent emitting material. Therefore, many high triplet energy HTMs have been synthesized. The most well known high triplet energy HTM is 1,3-di(9H-carbazol-9-yl)benzene (mCP) [1,2]. It has a high triplet energy of 2.9 eV and HOMO level of 6.1 eV for hole injection. However, poor thermal stability caused by low glass transition temperature limited its use as the high triplet energy HTM. Other than mCP, various carbazole or aromatic amine based HTMs have been reported [3–9]. However, there are only several high triplet energy HTMs which can be used in deep blue PHOLEDs. Therefore, further development of HTMs with high triplet energy above 2.80 eV is necessary to develop high efficiency deep blue PHOLEDs.

In this work, a novel high triplet energy HTM with an appropriate HOMO level, 4,4′-(10-phenyl-9,10-dihydroacridine-9,9-diyl)bis(*N*,*N*-diphenylaniline) (PADPA), was designed and synthesized as a HTM to obtain low driving voltage and high power efficiency for deep blue PHOLEDs. The synthesis and photophysical properties of PADPA are described and the device performances of deep blue PHOLEDs with PADPA HTM were investigated. It was demonstrated that PADPA can be effectively used as the HTM for low driving voltage and high power efficiency in deep blue PHOLEDs.

2. Experimental

The synthesis of intermediate compound and general analysis of synthesized compound are described in our previous work [10].

* Corresponding author. Tel./fax: +82 31 8005 3585.
E-mail address: leej17@dankook.ac.kr (J.Y. Lee).

1566-1199/$ - see front matter © 2012 Elsevier B.V. All rights reserved.
http://dx.doi.org/10.1016/j.orgel.2012.03.040

2.1. Synthesis of 4,4′-(10-phenyl-9,10-dihydroacridine-9,9-diyl)bis(N,N-diphenylaniline) (PADPA)

A 100 ml flask was charged with 9,9-bis(4-bromophenyl)-10-phenyl-9,10-dihydroacridine (0.6 g, 0.001 mol), diphenylamine (0.44 g, 0.002 mol), palladium(II) acetate (0.012 g, 0.00005 mol), and toluene (10 ml) under an argon atmosphere. A solution of sodium-t-butoxide (0.61 g, 0.0064 mol) in toluene (5 ml) and tri-tert-butylphosphine (1.27 ml, 1 M) were added slowly. The mixture was refluxed under an argon atmosphere for 10 h. After cooling the solution, the reaction mixture was extracted with diluted water and chloroform. The combined organic solution was dried over magnesium sulfate and concentrated. Purification by silicagel chromatography using chloroform/n-hexane gave a white powder. The product was obtained to 0.48 g (yield 61%). T_g 125 °C. ^{1}H-NMR (600 MHz, $CDCl_3$): δ7.55 (t, 2H, J = 18.0 Hz), 7.47(t, 1H, J = 12.0 Hz), 7.26–7.23(m, 8H), 7.12–7.09(m, 10H), 7.04(t, 2H, J = 12.0 Hz), 7.00–6.95(m, 10H), 6.90(t, 2H, J = 12.0 Hz), 6.85(d, 2H, J = 6.0 Hz), 6.44 (d, 2H, J = 12.0 Hz).^{13}C-NMR (600 MHz, $CDCl_3$): δ 148.1, 146.0, 142.4, 140.8, 131.8, 130.9, 130.4, 130.1, 128.9, 127.5, 125.1, 124.0, 122.4, 56.1. MS (FAB) miz 744 [$(M+H)^+$]. Anal. Calcd for $C_{55}H_{41}N_3$: C, 88.80; H, 5.55; N, 5.65. Found: C, 88.53; H, 5.46; N, 5.55.

2.2. Device fabrication

The device structure of blue PHOLEDs was indium tin oxide (ITO, 150 nm)/*N*,*N*′-diphenyl-*N*,*N*′-bis- [4-(phenyl-m-tolyl-amino)-phenyl]-biphenyl-4,4′-diamine (DNTPD, 60 nm)/*N*,*N*′-di(1-naphthyl)-*N*,*N*′-diphenylbenzidine(NPB, 5 nm)/PADPA or 1,1-bis[(di-4-tolylamino)phenyl]cyclohexane (TAPC) or 4,4′-(8H-indolo[3,2,1-de]acridine-8,8-diyl)bis(*N*,*N*-diphenylaniline) (FPCA) (10 nm)/9-(3-(9H-carbazole-9-yl)phenyl)-3-(dibromophenylphosphoryl)-9H-carbazole (mCPPO1):bis((3,5-difluoro-4-cyanophenyl)-pyridine) iridium picolinate (FCNIrpic)(30 nm, 3%)/diphenylphosphine oxide-4-(triphenylsilyl)phenyl (TSPO1, 25 nm)/LiF(1 nm)/Al(200 nm). All organic materials were deposited by vacuum thermal evaporation. All devices were encapsulated with a CaO getter and a glass lid after device fabrication. The device performances of the blue PHOLEDs were measured with Keithley 2400 source measurement unit and CS1000 spectroradiometer.

3. Results and discussion

PADPA was synthesized by the reaction of brominated triphenylamine with 4,4′-dibromobenzophenone followed by ring closing reaction using a strong acid and amination with diphenylamine [10]. Synthetic scheme of PADPA is shown in Scheme 1. PADPA was purified by a column chromatography and a high purity over 99% was obtained from a high performance liquid chromatography analysis. PADPA compound was confirmed by ^{1}H and ^{13}C nuclear magnetic resonance, mass and elemental analysis.

Photophysical properties of PADPA were studied using ultraviolet–visible (UV–Vis) and photoluminescence (PL) measurements. Low temperature PL measurement of PADPA was carried out in liquid nitrogen using tetrahydrofuran solution of PADPA. The solution PL sample was exposed to Xe-lamp at low temperature to obtain low temperature PL spectrum. UV–Vis and PL spectra of PADPA are shown in Fig. 1. PADPA showed strong π–π^* absorption peak of triphenylamine and acridine core at 300 nm. As can be seen in the molecular structure, PADPA has three triphenylamine units which are separated by sp^3 carbon. Conjugation of three triphenylamine units is not extended due to sp^3 carbon and only the absorption of triphenylamine was observed. The bandgap of PADPA could be calculated from the absorption edge of UV–Vis spectrum and was 3.62 eV. PL emission of PADPA was observed at 364 nm. Low temperature PL spectrum of PADPA was also analyzed to measure the triplet energy of PADPA. The triplet energy of PADPA was calculated from the first phosphorescent emission peak at 428 nm and was 2.89 eV, which was high enough for exciton blocking in deep blue PHOLEDs.

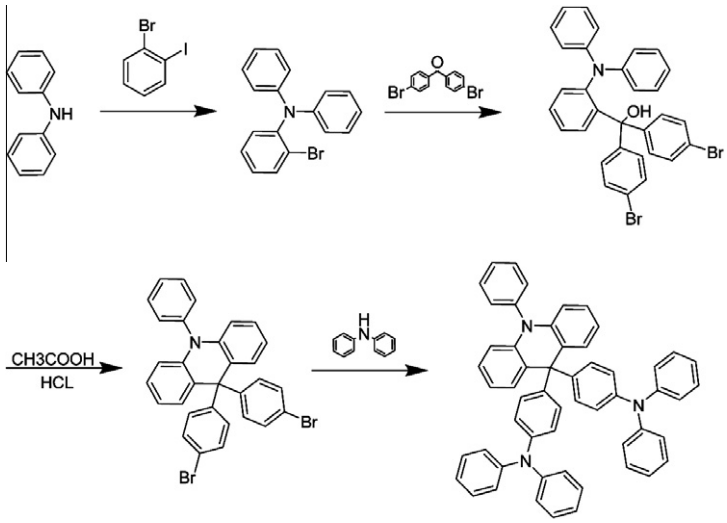

Scheme 1. Synthetic scheme of PADPA.

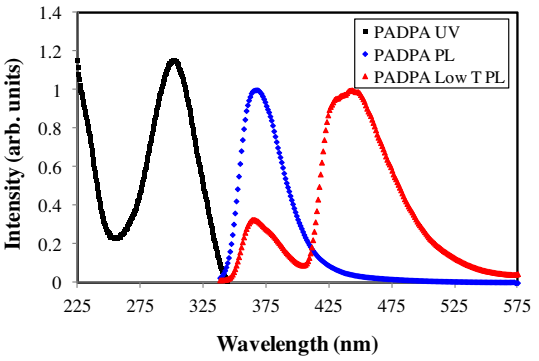

Fig. 1. UV–Vis and PL spectra of PADPA. Data were obtained in tetrahydrofuran solution at a concentration of 1.0×10^{-4} M. Low temperature PL measurement was carried out at 77 k.

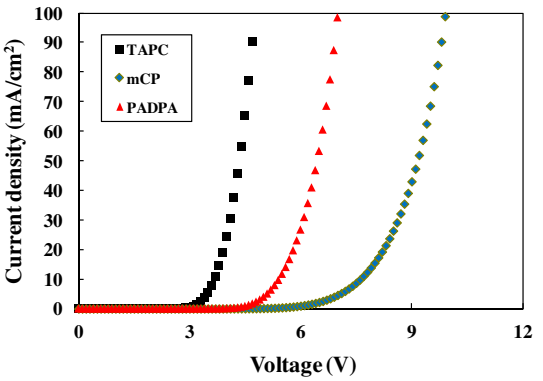

Fig. 3. Current density–voltage curves of PADPA, TAPC and mCP hole only devices.

Cyclic voltametry (CV) measurement of PADPA was carried out to measure the HOMO level. The HOMO level of PADPA was calculated to be −5.96 eV from the oxidation curve of CV measurement. The LUMO level of PADPA was −2.34 eV from the HOMO level and bandgap. The HOMO and LUMO levels of PADPA were suitable for hole injection into deep blue emitting layer and electron blocking from deep blue emitting layer, respectively. Therefore, PADPA can be effective as the HTM for deep blue PHOLEDs in terms of triplet exciton blocking, hole injection and electron blocking.

Molecular simulation of PADPA was performed to study the HOMO and LUMO distribution. Density functional theory calculation was carried out using a suite of Gaussian 03 program and the nonlocal density functional of Becke's 3-parameters employing Lee-Yang-Parr functional (B3LYP) with 6–31G* basis sets [11]. HOMO and LUMO distribution of PADPA is shown in Fig. 2. HOMO of PADPA was localized on the triphenylamine unit, while LUMO of PADPA was dispersed mostly over the acridine core due to strong electron donating character of the triphenylamine unit. We reported two acridine type core structures in our previous works [4,5]. Acridine based hole transport materials showed good device performances, but the problem of two acridine cores was the planarity of the core. As the whole core structure was in the same plane, excimer formation could be easily induced. The problem of planar molecular structure could be solved by designing a phenyl substituted acridine core because the phenyl unit attached to the acridine core is out of the acridine plane. Therefore, excimer or exciplex formation at the interface can be suppressed in PADPA device. This can be confirmed in the geometrical structure of PADPA in Fig. 2.

One merit of the acridine core is the rigidity because the molecular motion of the acridine unit is hindered by six-membered ring structure. The rigid fused ring structure can improve the glass transition temperature of PADPA and a high glass transition temperature of 125 °C was obtained from differential scanning calorimeter. Therefore, the poor thermal stability problem of mCP and other high triplet energy HTMs was solved by using PADPA as high triplet energy HTM.

Hole only device of PADPA was fabricated to study the hole transport properties of PADPA. TAPC and mCP were used as standard materials. Fig. 3 shows current density–voltage curves of hole only devices. Hole current density of PADPA device was higher than that of mCP device, while it was lower than that of TAPC device. It was reported that TAPC and mCP show hole mobilities of 1.0×10^{-2} cm^2/V s and 5×10^{-4} cm^2/V s, respectively [12,13]. Therefore, hole only device result indicates that PADPA shows a hole mobility between mCP mobility and TAPC mobility.

Deep blue PHOLEDs with PADPA as a HTM were fabricated to investigate the device performances of PADPA.

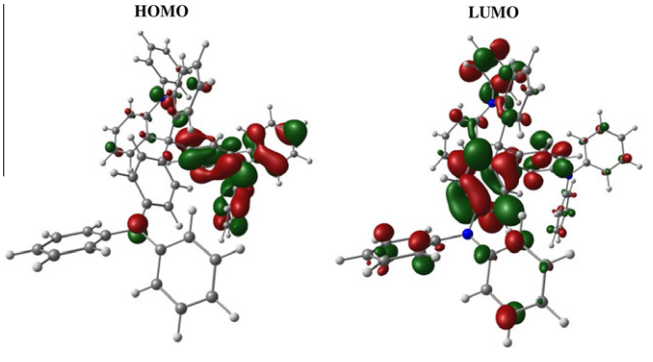

Fig. 2. HOMO and LUMO distribution of PADPA.

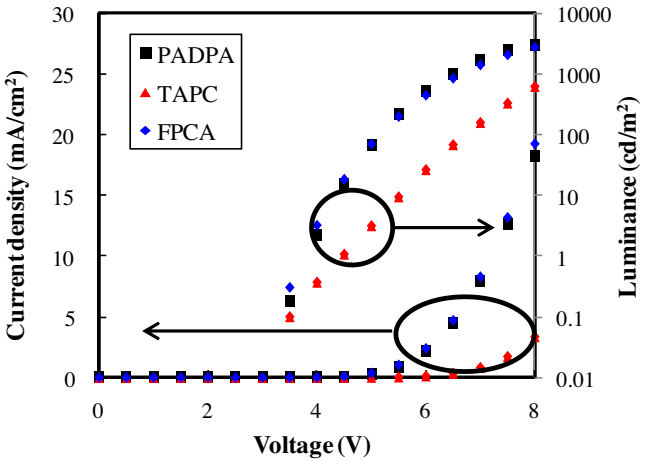

Fig. 4. Current density–voltage-luminance curves of blue PHOLEDs with TAPC, FPCA and PADPA hole transport layer.

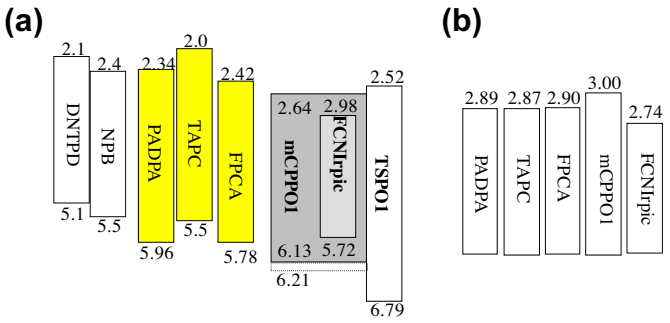

Fig. 5. Energy level diagram of deep blue PHOLEDs (a) and triplet energy of materials (b).

TAPC and FPCA were used as standard materials. Fig. 4 shows current density–voltage and luminance-voltage curves of PADPA, TAPC and FPCA based deep blue PHOLEDs. The current density and luminance of PADPA device were much higher than those of TAPC device and similar to those of FPCA at the same driving voltage. This indicates that PADPA is much better than TAPC and similar to FPCA to inject holes into mCPPO1:FCNIrpic emitting layer. In general, hole transport and injection properties of HTM affect the current density of the device. In the case of PADPA, the high current density is mostly due to improved hole injection properties. As can be seen in the energy level diagram of the device in Fig. 5, the energy barriers for hole injection from HTM to emitting layer are 0.17 and 0.63 eV for PADPA and TAPC, respectively. The large energy barrier for hole injection from TAPC to mCPPO1:FCNIrpic emitting layer limits hole current density in the emitting layer, resulting in low current density. Compared with TAPC device, the energy barrier for hole injection of PADPA device is only 0.17 eV, facilitating hole injection from PADPA to emitting layer. Therefore, high current density and low driving voltage were obtained in PADPA device.

Quantum efficiency–luminance curves of PADPA, TAPC and FPCA devices are shown in Fig. 6. The quantum efficiency of PADPA device was slightly higher than that of TAPC device and similar to that of FPCA device at the same luminance. The maximum quantum efficiency of PADPA device was 17.3% and the quantum efficiency at 1000 cd/m^2 was 15.3%. The high quantum efficiency of PADPA device is due to efficient hole injection effect. Efficient hole injection balanced holes and electrons in the emitting layer, resulting in high quantum efficiency in PADPA device. The high triplet energy of 2.89 eV of PADPA and 2.87 eV of TAPC similarly suppressed triplet exciton quenching of the emitting layer as reported in other works [14,15]. The quantum efficiency of PADPA device was comparable to that of FPCA device, indicating that PADPA is suitable as high triplet energy HTMs for deep blue PHOLED. The quantum efficiency of FPCA device was lower than that we reported in our earlier work because of low quantum efficiency of dopant material we used [4]. The quantum efficiency of TAPC device was also high due to high triplet energy of TAPC and electron blocking although the quantum efficiency was slightly lower than that of PADPA due to poor hole injection.

Power efficiency of PADPA device was compared with that of TAPC and FPCA devices (Fig. 7). The power efficiency of PADPA device was much higher than that of TAPC device and similar to that of FPCA device over all luminance range. The maximum power efficiency and power efficiency at

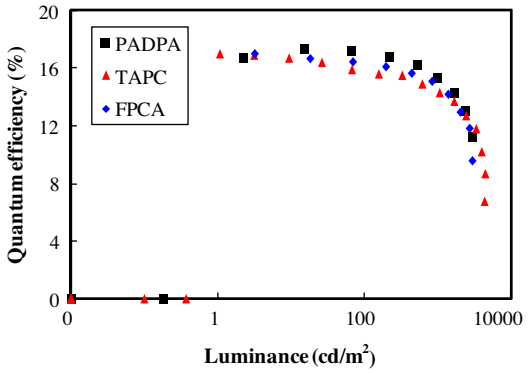

Fig. 6. Quantum efficiency–luminance curves of blue PHOLEDs with TAPC, FPCA and PADPA hole transport layer.

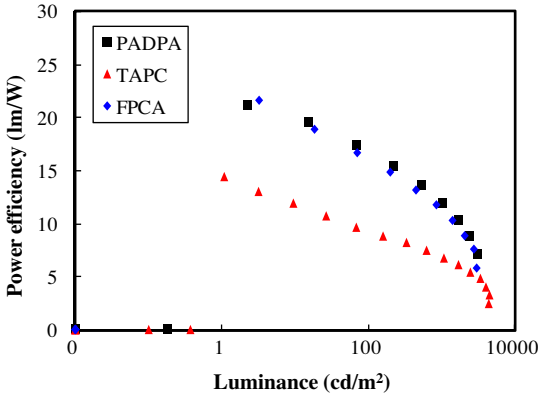

Fig. 7. Power efficiency–luminance curves of green PHOLEDs with TAPC, FPCA and PADPA hole transport layer.

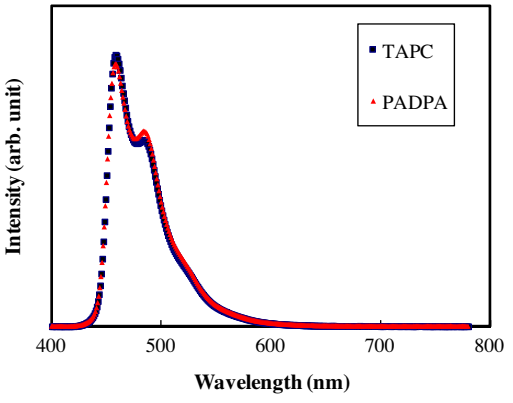

Fig. 8. EL spectra of TAPC and PADPA devices.

1000 cd/m^2 of PADPA device were 21.1 lm/W and 11.9 lm/W, respectively. However, TAPC device showed only maximum power efficiency of 14.4 lm/W and power efficiency at 1000 cd/m^2 of 6.8 lm/W. There was more than 50% improvement of power efficiency by replacing TAPC with PADPA. The improved power efficiency of PADPA device is mostly originated from the low driving voltage as shown in Fig. 4 because there was only small difference of quantum efficiency between PADPA and TAPC.

Electroluminescence (EL) spectrum of PADPA device are shown in Fig. 8. EL spectrum of TAPC device is also shown in this figure. Both devices showed deep blue emission spectrum with a emission peak at 458 nm. Color coordinates of PADPA and TAPC devices were (0.14, 0.19) and (0.14, 0.18), respectively.

4. Conclusions

In conclusion, an acridine based HTM, PADPA, was effectively synthesized as a HTM for deep blue PHOLEDs and improved the driving voltage and power efficiency of deep blue PHOLEDs. In particular, the power efficiency of deep blue PHOLEDs was enhanced by more than 50% using PADPA HTM. Therefore, the acridine core can be useful as the core of organic charge transport materials.

References

[1] R.J. Holmes, B.W. D'Andrade, S.R. Forrest, X. Ren, J. Li, M.E. Thompson, Appl. Phys. Lett. 83 (2003) 3818.
[2] K. Goushi, R. Kwong, J.J. Brown, H. Sasabe, C. Adachi, J. Appl. Phys. 95 (2004) 7798.
[3] N. Chopra, J. Lee, Y. Zheng, S.–H. Eom, J. Xue, F. So, Appl. Phys. Lett. 93 (2008) 143307.
[4] M.S. Park, J.Y. Lee, Chem. Mater. 23 (2011) 4338.
[5] M.S. Park, J.Y. Lee, J. Mater. Chem. 22 (2012) 3099.
[6] D. Tanaka, Y. Agata, T. Takeda, S. Watanabe, J. Kido, Jpn. J. Appl. Phys. 46 (2007) L117.
[7] Y. Agata, H. Shimizu, J. Kido, Chem. Lett. 36 (2007) 316.
[8] Y.J. Cho, J.Y. Lee, Adv. Mater. 23 (2011) 4568.
[9] M.T. Lee, J.S. Lin, M.T. Chu, M.R. Tseng, Appl. Phys. Lett. 94 (2009) 083506.
[10] M.G. Kim, J.Y. Lee, Chem. Asia J. (2012), http://dx.doi.org/10.1002/asia.201101030.
[11] M.J. Frisch, G.W. Trucks, H.B. Schlegel, G.E. Scuseria, M.A. Robb, J.R. Cheeseman, J.A. Montgomery, T. Vreven Jr., K.N. Kudin, J.C. Burant, J.M. Millam, S.S. Iyengar, J. Tomasi, V. Barone, B. Mennucci, M. Cossi, G. Scalmani, N. Rega, G.A. Petersson, H. Nakatsuji, M. Hada, M. Ehara, K. Toyota, R. Fukuda, J. Hasegawa, M. Ishida, T. Nakajima, Y. Honda, O. Kitao, H. Nakai, M. Klene, X. Li, J.E. Knox, H.P. Hratchian, J.B. Cross, C. Adamo, J. Jaramillo, R. Gomperts, R.E. Stratmann, O. Yazyev, A.J. Austin, R. Cammi, C. Pomelli, J.W. Ochterski, P.Y. Ayala, K. Morokuma, G.A. Voth, P. Salvador, J.J. Dannenberg, V.G. Zakrzewski, S. Dapprich, A.D. Daniels, M.C. Strain, O. Farkas, D.K. Malick, A.D. Rabuck, K. Raghavachari, J.B. Foresman, J.V. Ortiz, Q. Cui, A.G. Baboul, S. Clifford, J. Cioslowski, B.B. Stefanov, G. Liu, A. Liashenko, P. Piskorz, I. Komaromi, R.L. Martin, D.J. Fox, T. Keith, M.A. Al-Laham, C.Y. Peng, A. Nanayakkara, M. Challacombe, P.M.W. Gill, B. Johnson, W. Chen, M.W. Wong, C. Gonzalez, J.A. Pople, Gaussian 03, revision B05, Gaussian, Inc., Pittsburgh, PA, 2003.
[12] T. Tsuboi, S.-W. Liu, M.-F. Wu, C.-T. Chen, Org. Electron. 10 (2009) 1372.
[13] P. Strohriegl, J.V. Grazulevicius, Adv. Mater. 14 (2002) 1439.
[14] J. Lee, J.I. Lee, K. Song, S.J. Lee, H.Y. Chu, Appl. Phys. Lett. 92 (2008) 203305.
[15] N. Chopra, J. Lee, Y. Zheng, S. Eom, J. Xue, F. So, Appl. Phys. Lett. 93 (2008) 143307.